[15] Z. F. Ren, Z. P. Huang, D. Z. Wang, J. G. Wen, J. W. Xu, J. H. Wang, L. E. Calvet, J. Chen, J. F. Klemic, M. A. Reed, *Appl. Phys. Lett.* **1999**, *75*, 1086.
[16] J. Bonard, P. Chauvin, C. Klinke, *Nano Lett.* **2002**, *2*, 665.
[17] a) F. S. Bates, *Science* **1991**, *251*, 898. b) F. S. Bates, G. H. Fredrickson, *Annu. Rev. Phys. Chem.* **1990**, *41*, 525.
[18] L. Leibler, *Macromolecules* **1980**, *13*, 1602.
[19] C. Park, J. Yoon, E. L. Thomas, *Polymer* **2003**, *44*, 6725.
[20] I. W. Hamley, *Nanotechnology* **2003**, *14*, R39.
[21] a) M. Park, C. Harrison, P. M. Chaikin, R. A. Register, D. H. Adamson, *Science* **1997**, *276*, 1401. b) M. Park, P. M. Chaikin, R. A. Register, D. H. Adamson, *Appl. Phys. Lett.* **2001**, *79*, 257.
[22] a) J. P. Spatz, P. Eibeck, S. Mößmer, M. Möller, T. Herzog, P. Ziemann, *Adv. Mater.* **1998**, *10*, 849. b) J. P. Spatz, T. Herzog, S. Mößmer, P. Ziemann, M. Möller, *Adv. Mater.* **1999**, *11*, 149.
[23] T. Xu, J. Stevens, J. Villa, J. T. Goldbach, K. W. Guarini, C. T. Black, C. J. Hawker, T. P. Russell, *Adv. Funct. Mater.* **2003**, *13*, 698.
[24] T. Thurn-Albrecht, J. Schotter, G. A. Kästle, N. Emley, T. Shibauchi, L. Krusin-Elbaum, K. Guarini, C. T. Black, M. T. Tuominen, T. P. Russell, *Science* **2000**, *290*, 2126.
[25] W. A. Lopes, H. M. Jaeger, *Nature* **2001**, *414*, 735.
[26] For a recent review on poly(ferrocenylsilanes) see: K. Kulbaba, I. Manners, *Macromol. Rapid Commun.* **2001**, *22*, 711.
[27] R. G. H. Lammertink, M. A. Hempenius, G. J. Vancso, *Langmuir* **2000**, *16*, 6245.
[28] R. G. H. Lammertink, M. A. Hempenius, G. J. Vancso, K. Shin, M. H. Rafailovich, J. Sokolov, *Macromolecules* **2001**, *34*, 942.
[29] R. G. H. Lammertink, M. A. Hempenius, V. Z.-H. Chan, E. L. Thomas, G. J. Vancso, *Chem. Mater.* **2001**, *13*, 429.
[30] a) R. G. H. Lammertink, M. A. Hempenius, J. E. Van den Enk, V. Z.-H. Chan, E. L. Thomas, G. J. Vancso, *Adv. Mater.* **2000**, *12*, 98. b) L. Cao, J. A. Massey, M. A. Winnik, I. Manners, S. Rieth Müller, F. Banhart, J. P. Spatz, M. Möller, *Adv. Funct. Mater.* **2003**, *13*, 271.
[31] J. Y. Cheng, C. A. Ross, E. L. Thomas, H. I. Smith, G. J. Vancso, *Appl. Phys. Lett.* **2002**, *81*, 3657.
[32] J. Y. Cheng, C. A. Ross, V. Z.-H. Chan, E. L. Thomas, R. G. H. Lammertink, G. J. Vancso, *Adv. Mater.* **2001**, *13*, 1174.
[33] Y. Ni, R. Rulkens, I. Manners, *J. Am. Chem. Soc.* **1996**, *118*, 4102.
[34] Like other block copolymers containing mutually immiscible blocks, PS–PFS block copolymers microphase separate to form a variety of morphologies in bulk: R. G. H. Lammertink, M. A. Hempenius, E. L. Thomas, G. J. Vancso, *J. Polym. Sci., Part B: Polym. Phys.* **1999**, *37*, 1009.
[35] T. Lin, G. Seshadri, F. A. Keller, *Appl. Surf. Sci.* **1997**, *119*, 83.
[36] T. Deng, Y. Ha, J. Y. Cheng, C. A. Ross, E. L. Thomas, *Langmuir* **2002**, *18*, 6719.
[37] J. Y. Cheng, C. A. Ross, E. L. Thomas, H. I. Smith, G. J. Vancso, *Adv. Mater.* **2003**, *15*, 1599.
[38] For other work on inducing long-range order in block copolymer thin films by topographically patterned substrates see: a) R. A. Segalman, H. Yokoyama, E. J. Kramer, *Adv. Mater.* **2001**, *13*, 1152. b) R. A. Segalman, A. Hexemer, E. J. Kramer, *Macromolecules* **2003**, *36*, 6831.

# How Polycrystalline Devices Can Outperform Single-Crystal Ones: Thin Film CdTe/CdS Solar Cells**

By *Iris Visoly-Fisher*, *Sidney R. Cohen*, *Arie Ruzin*, and *David Cahen**

Using lower quality materials yields cheaper devices, but normally this decreases device performance. Optoelectronic devices, based on single-crystal semiconductor physics, are expected to display peak performance if fabricated with perfect crystals. Polycrystalline (PX) materials are mostly characterized by two-dimensional (2D) defects, grain boundaries (GBs), and grain surfaces. However, several types of thin film PX solar cells outperform their single-crystal analogues.[1] The question is, why? The defect density within the grains may be reduced by "gettering" of defects and impurities at the GBs, but GBs are also expected to decrease device efficiency. This is due to the enhanced recombination of photo-generated charge carriers at GBs.[1] Our results, from high-resolution characterization of CdTe/CdS PX solar cells, indicate that CdTe GBs do *not* enhance recombination, but rather participate in the photovoltaic energy conversion process as efficient photocurrent collectors and transporters. This suggests that structural defects can be advantageous for device performance, if properly designed, even in devices whose operation is based on physics of ideal, perfect solids.

Photovoltaic action includes photogeneration of electronic charges, their separation, transport and, ultimately, collection at electrodes. Crystal defects and impurities at the GBs, present in PX semiconductors, can trap and localize charges. Such charges then induce regions depleted of majority charge carriers near the GB, causing an electrostatic potential barrier (band bending) for transport of majority carriers across

[*] Prof. D. Cahen, I. Visoly-Fisher, Dr. S. R. Cohen
Weizmann Institute of Science
Rehovot 76100 (Israel)
E-mail: david.cahen@weizmann.ac.il
Dr. A. Ruzin
Dept. of Physical Electronics, Tel Aviv University
Tel Aviv 69978 (Israel)

[**] We thank L. Kronik (WIS) for many helpful discussions, P. De Wolf (Veeco) for guidance with SCM, S. Richter (TAU) for guidance with CP-AFM, V. Kaydanov (Col. School of Mines) for discussions, I. Bar-Yosef (WIS) for use of the Dimension microscope, USDOE (via NREL) for initial, and the Weizmann Institute's Levin fund (DC) and Feinberg Grad. School (IVF)) for further support. DC holds the Schaefer Chair in Energy Research. Most of the results that are presented here, as well as the basic model, were reported at the Spring 2003 (April 21–25) MRS meeting (S. Francisco, Symp. B; cf. also *MRS Bull.* **2003**, *28(7)*, 521) and at the *38th IUVSTA and ISF Workshop on Electronic Processes and Sensing on the Nano-Scale* (Eilat, May 25–29, 2003). Subsequently Persson & Zunger reported electronic structure calculations (*Phys. Rev. Lett.* **2003**, *91*, 266 401), which they used to promote an explanation for the superiority of PX $CuInSe_2$ solar cells. Their model – charge separation near, and transport at, GBs – conforms closely to ours.


DOI: 10.1002/adma.200306624

ADVANCED MATERIALS

GBs.[2] In solar cells, GBs can decrease the photogenerated current further by enhancing recombination of photogenerated carriers via localized energy states.[3] Still, several types of PX solar cells show such high photocurrents that one can question if current collection is really limited by grain bulk, surface, and/or GBs. To answer that, we explored ways of characterizing the electrical properties of single GBs and grain surfaces of the ~1 μm sized CdTe grains in p-CdTe/n-CdS PX thin film solar cells.

Characterizing a single GB obviates the need to average over different GB lengths and crystal orientations, as is done when processing data from macroscopic measurements of PX materials.[4–6] Measurements of GBs within a device structure that underwent the entire cell manufacturing process should give more representative data than those on model systems (e.g., a single GB in a bicrystal).[7] The small grain size (~1 μm) does not allow the use of microcontacts, commonly used for electronic measurements of a single GB.[8] The major obstacle is to obtain, notwithstanding the rough PX topography, reproducible, interpretable, and representative results with minimal sample preparation. As explained elsewhere,[9] scanning capacitance microscopy (SCM), preferably in combination with scanning Kelvin probe microscopy (SKPM), can serve to characterize a single GB and grain surface electrically. The SCM signal is related to the type and concentration of majority charge carriers near the semiconductor surface.[10] SCM and topography maps are acquired simultaneously by atomic force microscopy, AFM, in contact mode. In this way the observed variations in carrier concentration can be related to structural features, such as GBs. In SKPM, a conductive AFM tip in non-contact mode serves to create a surface potential map.[9,11] Conductive probe AFM, CP-AFM, allows direct mapping of currents through single grains and GBs in contact mode. Our results represent the electronic properties under illumination, close to the real solar cell working conditions. This is because the 670 nm (1.85 eV) laser light used for the AFM (tip height) detection is reflected between tip and (rough CdTe) surface and absorbed by CdTe, which has a 1.45 eV absorption edge.

Our initial results,[9] from SCM and SKPM measurements, confirm the model of depleted GBs.[2] We thus find that there is a barrier for hole transport across GBs (with variations in barrier height between different boundaries), in agreement with models based on macroscopic transport measurements in such CdTe films.[4,5,7] Romero et al. also interpret cathodoluminescence mapping results by an increased density of impurity-related states at GBs, resulting in an electric fields surrounding the GBs.[12] However, the question "why do the cells work so well?" remains open. We will show below that the answer can be connected to enhanced separation and collection of photogenerated charge carriers by CdTe GBs, due to GB properties that were induced by the post-deposition heat-treatment in $CdCl_2$.

The CdTe GB core properties were characterized using the higher resolution of CP-AFM, compared to the SCM and SKPM measurements described above. At zero bias, CP-AFM will map photovoltaic currents (Fig. 1a), induced by separation of the electron–hole pairs photogenerated by the AFM laser light, in the cell's junction field. The strong effect of the AFM laser was verified by separate measurements with

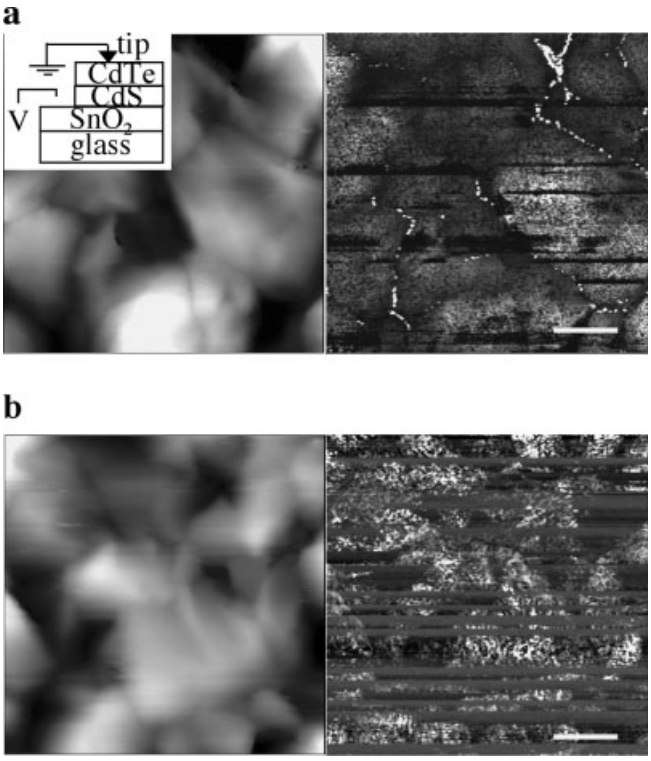


**Figure 1.** Simultaneously collected a) atomic force microscopy (AFM) topography (left), and conductive probe AFM (CP-AFM) current mapping (right), images of the polycrystalline CdTe surface of $CdCl_2$-treated CdTe/CdS cell. Brighter CP-AFM signal indicates larger current. b) Topography (left) and CP-AFM (right) images of CdTe surface in a non-$CdCl_2$ treated cell. As no external bias was applied, CP-AFM mapped the photocurrents induced by the AFM laser. Image sizes 5 μm × 5 μm. *Z* range: topography images, 500 nm; current mapping, 150 pA. The bar indicates 1 μm.

an external light source, which had a very small (or no) effect on the results.[13] If the cell is connected in a circuit, i.e., by the tip and the $SnO_2$ (inset of Fig. 1a), the resulting current can be collected and measured. Consistent with the SCM results, the photovoltaic current maps show decreased currents close to the GBs, within 200–350 nm from the GB core. Surprisingly, though, high currents are seen in the cores of most GBs (Fig. 1a).

These GB core currents are postulated to be minority carrier currents, i.e., of photogenerated electrons in the p-CdTe, which flow opposite to the junction field's direction and are collected by the $SnO_2$ electrode. The photogenerated hole counterparts would then be transported via the grain bulk, in an opposite process, and collected at the back contact. Collection of electrons generated near the CdTe surface, via grain bulk, follows one-dimensional photovoltaic physics, with regard to the wide depletion layer in CdTe (due to low p-doping), and allows electron transport to the p–n junction and col-

  

lection at the $SnO_2$ electrode. However, near a GB, the photogenerated electrons are drawn into the GB core by the GB band bending, as deduced from SCM and SKPM. Therefore, the current collected near the GBs is reduced. The increased currents in the GB cores result from the (photogenerated) electrons confined there, flowing along the GB core, and indicate the absence of significant recombination there. This is consistent with inversion at the GB core, which implies the scarcity of free holes to recombine with the electrons. Sheet conduction along GBs was also suggested as occurring in InSb thin films,[14] and as a possible explanation for the observed electrical properties of PX CdTe surface barrier diodes.[15] We note that the photogenerated holes would have to cross some GB barriers to arrive at the back contact, a process whose driving force is the elimination of charging of CdTe by the efficient collection of the electron at the other (n-type) end of the photovoltaic junction.

As noted above, SCM showed hole depletion near GBs, expressed by a brighter SCM signal (see Cahen and co-workers[9] and Fig. 2a). The width of the GB hole depletion region varied from 100 to 300 nm in different GBs, indicating differences in the barrier height resulting from different crystal orientations of the grains, and possibly also from different impurity content in different GBs. SKPM showed a smaller work function at GBs than at outer CdTe grain surfaces (not shown). Based on the SCM we conclude that this work function reduction is related to depletion of holes near the GB, rather than an artifact related to convolution with topography.[9] Support for GB inversion comes from SCM performed with sharper tips, showing darker lines at several GB cores (Fig. 2a, bottom left corner of right panel),[16] i.e., SCM signals close to zero, typical of an insulating material. This is consistent with an inverted GB core (no free holes). The signal is not exactly zero due to the limited resolution of SCM, which convolutes signals from the GB core and the adjacent depleted regions.

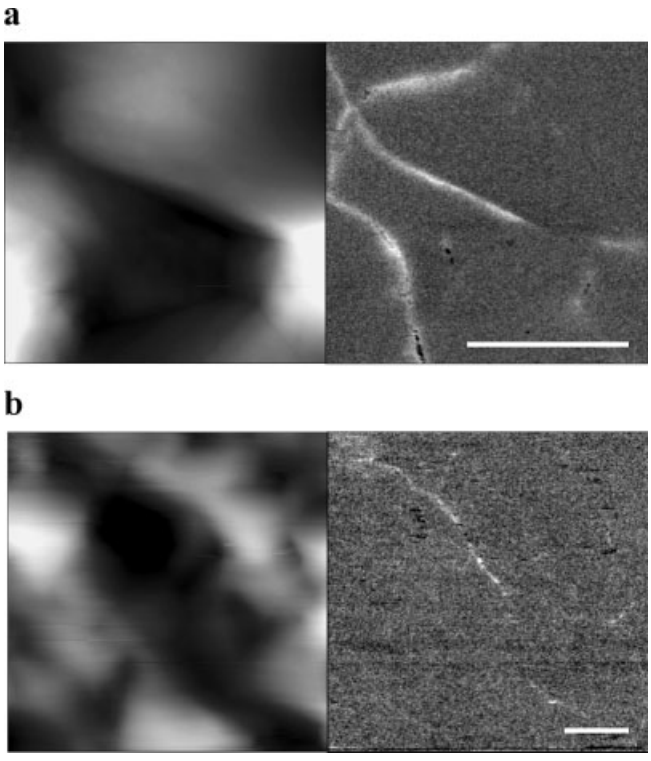


**Figure 2.** a) Simultaneously collected AFM topography image (left) and scanning capacitance microscopy (SCM) image (right) of polycrystalline CdTe surface of $CdCl_2$-treated CdTe/CdS cell. Image size 2 μm × 2 μm. b) Topography (left) and SCM (right) images of CdTe surface in a non-$CdCl_2$ treated cell. Image size 5 μm × 5 μm. Topography *Z* range: 500 nm. The bars indicate 1 μm.

Why would the GB be inverted? Cl, found in higher concentrations at GBs,[17,18] can create $Cl_{Te}$ donor surface defects,[19] which will lead to further inversion, if the donor concentration at the GBs is high enough so that it is not neutralized by $O_{Te}$ acceptors.[20] Doping CdTe with Cl was found to induce n-type behavior with carrier concentration of $2 \times 10^{18}$ $cm^{-3}$,[21] and compensation by Cd from the $CdCl_2$ should be negligible, as deduced from comparison to doping with $CdI_2$.[22] Inversion requires a band bending of 0.5 V to have the Fermi level at midgap in the GB core. Such band bending within the 300 nm GB depletion region requires a $\sim 7 \times 10^{15}$ $cm^{-3}$ doping level in the CdTe grain bulk (using the one-sided abrupt junction approximation).[23] This is just one order of magnitude larger than the average value, deduced from transport measurements in CdTe films ($7 \times 10^{14}$ $cm^{-3}$).[5] This small discrepancy probably originates from the averaging nature of macroscopic measurements, which does not take into account possible differences between one grain/GB to another.

Support for inversion at GBs due to Cl comes from comparison of CdTe/CdS cells before and after heating the cells with $CdCl_2$ in air. This treatment is known to improve the cell performance.[24] $CdCl_2$-treated cells showed (by SCM) much stronger GB hole depletion than untreated cells (Figs. 2a,b), indicating that $CdCl_2$ increases hole depletion near the GBs. We note that CdTe GBs were found by Woods et al. to be inverted even before $CdCl_2$ treatment.[6] However, their results support our model in the sense that they indicate an increase in GB band bending after $CdCl_2$ treatment.[6] While CP-AFM shows significant GB core currents in $CdCl_2$-treated cells (Fig. 1a), these are mostly absent in untreated cells (Fig. 1b). Additionally, the GB depletion widths were narrower in the untreated cells (100–250 nm, from CP-AFM images of several similar samples; not shown) than in the $CdCl_2$-treated ones (200–350 nm). Because of the known positive effect of $CdCl_2$ treatment on CdTe/CdS cell performance, this suggests that the GB electronic structure induced by $CdCl_2$ treatment is beneficial for good cell performance. The similar topographical roughness of untreated and $CdCl_2$-treated cells eliminates the possibility that contact-area changes can explain the GB core currents, seen only in the $CdCl_2$-treated cells. Similarly, changes in the observed width of the depletion layer in SCM, between $CdCl_2$-treated and untreated samples, exclude tip contact area-related issues in that measurement.

  

ADVANCED MATERIALS

Thus, we arrive at the following mechanism to explain the superiority of these polycrystalline devices over single-crystal ones. GBs improve cell properties because of processes that evolve during the $CdCl_2$ treatment. Not only is the crystalline quality of the grains improved by gettering of defects and impurities into GBs[1] (it is well known that growth of high-quality large CdTe crystals from the melt is difficult),[25] but additionally the unique doping profile that forms near GBs is beneficial for cell performance. The latter can be understood by separation of photogenerated electron–hole pairs in the potential gradient of the GB depletion layer, which normally only occurs near the photovoltaic junction. The electrons are drawn into the GB core and flow along GBs towards the junction, while holes are transported through the grain bulk towards the back contact. Figure 3 shows these processes schematically. This charge separation, along with reduced recombination in the grain bulk (due to reduced defect concentration) and in GBs (as shown by CP-AFM) leads to a reduction in the overall recombination in the cell, and improved collection of photogenerated carriers.[26,27] Enhanced collection of photogenerated minority carriers by CdTe GBs was also suggested by Meyers and Albright.[28] SCM and SKPM cross-section mapping shows no evidence for a buried homojunction in these PX cells.[29] This is important because if there were a homojunction inside the grain, the GBs would cross the junction, and transport along GBs would harm cell performance (by shunting). However, in our case, the CdTe GB–CdS contact is an $n^-$–$n^+$ junction, which can behave as a photovoltaic junction, though with a reduced junction barrier, which would limit the photovoltage of the cell (see also endnote[26]).

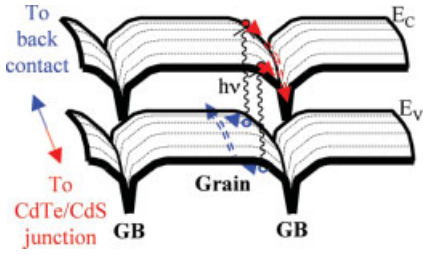


**Figure 3.** Schematic illustration of electron energy (vertical) versus spatial (horizontal) coordinate of CdTe grains in the solar cell, with the CdS in front of the plane of the paper. Blue/red circles show hole/electrons, and blue/red arrows show their direction of movement, respectively. $E_C$ and $E_V$ stand for the conduction band bottom and the valence band top, respectively. The scheme illustrates: proposed electronic energy variations near CdTe GBs; resulting separation of photogenerated electron–hole pairs near GBs; "funneling" of electrons into and their channeling along GB core.

There are some similarities between the role of GBs in CdTe and in Si absorber materials: GBs also act as a sink for impurities in Si cells, improving the quality of the grain bulk[1] (but, still, the quality of single-crystal Si is better). Enhanced P diffusion along GBs in columnar PX-Si structures induces an extension of the emitter layer along GBs, with charge separation occurring along these GBs.[30] In addition, a network of inversion channels was found in "ribbon growth on substrate" Si solar cells, consisting of densely packed precipitates around dislocations.[31] These channels collect minority carriers in the absorber part of the cell and lead them to the pn junction, thus increasing the cell's short-circuit current and decreasing open-circuit voltage.[32] Though the this type of structural defect is different from GBs, the observed properties are still quite similar.

Our results show that optimized solar cell absorber material can be polycrystalline, if the GBs are tailored to assist in photo-generated charge separation and transport. Other examples where defects improve device performance are known. Thus, in GaN devices GBs have been suggested as the cause of the high ultraviolet photoresponse gain and of the large optical gain required for lasing.[33] Controlled use of point defects was suggested to improve single crystal Si solar cell performance by creating an impurity band,[34] and vortex pinning in type II superconductors by defects can increase the critical current.[35] These (and other) examples suggest that defects need not be harmful, but may actually be beneficial for device performance.[36] Defect-assisted improvement of material properties can, thus, widen the pool of new materials for certain devices.

## *Experimental*

*CdTe/CdS Cells*: Most state-of-the-art cell structures (without contact to the p-CdTe) were provided by C. Ferekides (Univ. S. Florida), with the following layer sequence (Fig. 1a, inset): 7059 glass substrate/800–1000 nm transparent conductive oxide $SnO_2$:F/80–100 nm PX n-CdS/3–7 μm PX p-CdTe. CdS was deposited by chemical bath deposition, followed by closed-space vapor transport of the CdTe layer and $CdCl_2$-vapor treatment at 400 °C [37]. The samples were sonicated in de-ionized water (10 min) to remove residual $CdCl_2$, then etched with 0.1 % v/v $Br_2$/methanol for 10–20 s to remove the surface oxide, washed in methanol, and dried in a $N_2$ stream. Similar results are obtained with cell structures from First Solar (see [29] for structure details about the First Solar samples).

The difference in SCM and CP-AFM signals between GB and grain surface is explained by a change in the depleted layer at the grain surfaces (induced initially by the $CdCl_2$ treatment) by $Br_2$/methanol etching, which does not occur at the GBs. In contrast to the surface, the effect of $Br_2$/methanol etching on GBs is minimal [38]. This etching of the grain surface is important for making a low-resistance back contact to CdTe [39]. Hence, the grain surface and GB chemistry should be independently tailored for optimal cell performance, as was deduced earlier also for Cu(In,Ga)$Se_2$/CdS cells [40].

*SCM, SKPM, and CP-AFM*: In SCM the exact relation between signal magnitude and carrier concentration depends on measurement details, and was determined by comparison with reference samples. A positive signal (brighter than a reference) corresponds to p-type material; the brighter the signal, the lower the hole concentration. To avoid measuring SCM signals dependent on the distant cell junction, we measured with the junction under forward bias ($< -1$ V), where it does not contribute to the measured capacitance. We used a Dimension 3100 (DI-Veeco, Santa Barbara), equipped for SCM. The samples were biased via the $SnO_2$ (see Fig. 1a, inset). SCM measurements were found to be almost unaffected by surface topography [9]. SKPM was done on a P47 Solver Scanning Probe microscope (NT-MDT, Zelenograd). To minimize the convolution of rough topographic and electronic data, due to the involvement of long-range electrostatic

  

forces [11], a two-pass technique was used for the measurements [9]. CP-AFM was performed on a Dimension 3100 equipped with Tunneling AFM (TUNA) current amplifier. The bias was applied to the sample via the $SnO_2$ contact, as in SCM. Current mapping was done in the same bias range used for current–voltage measurements of CdTe/CdS solar cells (–1.5–0.5 V). The changes in the current with bias generally followed those observed in cells, i.e., the current reversed direction near the open-circuit voltage (~0.7 V) [39]. We used $PtIr_5$-coated Si probes (Nanosensors) with a typical tip radius of 25 nm, or Pt-coated Si probes (Micromasch) with tip radius of 35 nm. The lateral resolution of SCM is comparable to the tip radius [10]. The lateral resolution of CP-AFM is determined by the radius of the tip–surface contact area. Its minimum limit can be calculated by assuming a flat sample surface with Hertz theory [41]. Using a tip load of 100 nN, a tip radius of 25 nm and the mechanical constants of CdTe [25], this radius would be about 5 nm. The actual resolution in our case will be poorer because of the surface roughness. SKPM resolution is estimated to be about 100 nm, due to the effect of long-range electrostatic forces [42].

For SCM the CdTe surface oxide was re-grown by storage in room ambient for 48 h (~4 nm thick oxide) [43]. CP-AFM and SKPM mapping was done 24 h after etching, but no significant change in the results was noted even 14 days later. As all scanning probe mapping was done in air, it represents the electronic properties of the CdTe below the thin native oxide layer, assuming the oxide is not polar.

The similar topographical roughness of untreated and treated cells (Fig. 1a,b left), and the agreement with SCM data, eliminate the possibility of topography-induced artifacts to explain the GB core currents, seen only in the $CdCl_2$-treated cells.

Received: December 13, 2003
Final version: March 25, 2004
Published online: May 11, 2004

[1] H. J. Möller, *Semiconductors for Solar Cells*, Artech, Boston, MA **1993**.
[2] J. Y. W. Seto, *J. Appl. Phys.* **1975**, *46*, 5247.
[3] A. L. Fahrenbruch, R. H. Bube, *Fundamentals of Solar Cells: Photovoltaic Solar Energy Conversion*, Academic, New York **1983**.
[4] O. Vigil-Galán, L. Valliant, R. Mendoza-Pérez, G. Contreras-Puente, J. Vidal-Larramendi, *J. Appl. Phys.* **2001**, *90*, 3427.
[5] L. M. Woods, D. H. Levi, V. Kaydanov, G. Y. Robinson, R. K. Ahrenkiel, in *Proc. of 2nd World Conference on Photovoltaic Solar Energy Conversion*, Vol. 1 (Eds: J. Schmid, H. A. Ossenbrink, P. Helm, H. Ehmann, E. D. Dunlop), European Commission, Ispra, Italy **1998**, p. 1043.
[6] L. M. Woods, G. Y. Robinson, D. H. Levi, in *Proc. of 28th IEEE Photovoltaic Specialists Conference*, IEEE, Piscataway, NJ **2000**, p. 603.
[7] T. P. Thorpe, Jr., A. L. Fahrenbruch, R. H. Bube, *J. Appl. Phys.* **1986**, *60*, 3622.
[8] J. Fleig, S. Rodewald, J. Maier, *Solid State Ionics* **2000**, *136–137*, 905.
[9] I. Visoly-Fisher, S. R. Cohen, D. Cahen, *Appl. Phys. Lett.* **2003**, *82*, 556.
[10] C. C. Williams, *Ann. Rev. Mater. Sci.* **1999**, *29*, 471.
[11] A. Efimov, S. R. Cohen, *J. Vac. Sci. Technol. A* **2000**, *18*, 1051.
[12] M. J. Romero, M. M. Al-Jassim, R. G. Dhere, F. S. Hasoon, M. A. Contreras, T. A. Gessert, H. R. Moutinho, *Prog. Photovolt.: Res. Appl.* **2002**, *10*, 445.
[13] To be published.
[14] J. Shigeta, N. Kotera, T. Oi, *J. Appl. Phys.* **1976**, *47*, 621.
[15] L. A. Kosyachenko, V. M. Skylarchuk, Y. F. Skylarchuk, K. S. Ulyanitsky, *Solid State Phenom.* **1999**, *67–68*, 315.
[16] Such dark SCM lines in the GB core were not seen in all samples. We ascribe the differences between samples to possible differences in the $CdCl_2$ treatment, which affects the GB potential.
[17] B. E. McCandless, in *II-VI Compound Semiconductor Photovoltaic Materials, MRS Symp. Proc.*, Vol. 668 (Eds: R. Birkmire, R. Noufi, D. Lincot, H.-W. Schock), MRS, Warrendale, PA **2001**, H1.6.1.
[18] M. Terheggen, H. Heinrich, G. Kostorz, A. Romeo, D. Baetzner, A. N. Tiwari, A. Bosio, N. Romeo, *Thin Solid Films* **2003**, *431–432*, 262.
[19] K. Zanio, "Cadmium Telluride" (Eds: R. K. Willardson, A. C. Beer), in *Semiconductors and Semimetals*, Vol. 13, Academic, New York **1978**.
[20] D. Cahen, R. Noufi, *Appl. Phys. Lett.* **1989**, *54*, 558.
[21] D. Hommel, S. Scholl, T. A. Kuhn, W. Ossau, A. Waag, G. Landwehr, G. Bilger, *Mater. Sci. Eng. B* **1993**, *16*, 178.
[22] Y. Marfaing, *Thin Solid Films* **2001**, *387*, 123.
[23] S. M. Sze, *Physics of Semiconductor Devices*, Wiley, New York **1981**.
[24] K. Nakamura, M. Gotoh, T. Fujihara, T. Toyama, H. Okamoto, in *II-VI Compound Semiconductor Photovoltaic Materials, MRS Symp. Proc.*, Vol. 668 (Eds: R. Birkmire, R. Noufi, D. Lincot, H.-W. Schock), MRS, Warrandale, PA **2001**, H6.3.1.
[25] H. Hartmann, R. Mach, B. Selle, in *Current Topics in Materials Science,* Vol. 9 (Ed: E. Kaldis), North Holland, Amsterdam, **1982**, p. 1.
[26] According to our model one can argue that increased GB density (by reduced grain size) is beneficial. However, depleted/inverted GBs, ending at the cells' junction, would limit the photovoltage of the cell due to reduced junction barrier height in the depleted volume adjacent to the inverted GBs. Also, as the grains are isotropic in high efficiency CdTe cells, holes would have to cross some GB barriers to arrive at the back contact. Therefore, grain size should be optimized.
[27] We note that, especially in the last one and a half decades, PX CdTe/CdS solar cells were extensively empirically optimized for improved performance, while the problems encountered in improving single-crystal CdTe/CdS cells led to a decline in research with them. Irrespective of that, the difficulty in growing high PV quality single CdTe crystals will always limit the achievable efficiency of single-crystal cells.
[28] P. V. Meyers, S. P. Albright, *Prog. Photovolt.: Res. Appl.* **2000**, *8*, 161.
[29] I. Visoly-Fisher, S. R. Cohen, D. Cahen, C. S. Ferekides, *Appl. Phys. Lett.* **2003**, *83*, 4924.
[30] E. Christoffel, M. Rusu, A. Zegra, S. Bourdais, S. Noël, A. Slaoui, *Thin Solid Films* **2002**, *403–404*, 258.
[31] O. Breitenstein, M. Langenkamp, J. P. Rakotoniaina, *Diffus. Defect Data, Pt. B* **2001**, *78–79*, 29.
[32] T. Buonassisi, O. F. Vyvenko, A. A. Istratov, E. R. Weber, G. Hahn, D. Sontag, J. P. Rakotoniaina, O. Breitenstein, J. Isenberg, R. Schindler, *J. Appl. Phys.* **2004**, *95*, 1556.
[33] J. Salzman, C. Uzan-Saguy, B. Meyler, R. Kalish, *Phys. Status Solidi A* **1999**, *176*, 683.
[34] M. A. Green, *Prog. Photovolt.: Res. Appl.* **2001**, *9*, 137.
[35] J. I. Gersten, F. W. Smith, *The Physics and Chemistry of Materials*, Wiley, New York **2001**.
[36] The underlying concept here is profoundly different from that of devices whose function relies on the presence of structural defects (e.g., varistors).
[37] C. S. Ferekides, D. Marinsky, V. Viswanathan, B. Tetali, V. Palekis, P. Selvaraj, D. L. Morel, *Thin Solid Films* **2000**, *361–362*, 520.
[38] D. L. Baetzner, R. Wendt, A. Romeo, H. Zogg, A. N. Tiwari, *Thin Solid Films* **2000**, *361–362*, 463.
[39] K. Durose, P. R. Edwards, D. P. Halliday, *J. Cryst. Growth* **1999**, *197*, 733.
[40] L. Kronik, U. Rau, J.-F. Guillemoles, D. Braunger, H.-W. Schock, D. Cahen, *Thin Solid Films* **2000**, *361–362*, 353.
[41] S. R. Cohen, G. Neubauer, G. M. McClelland, *J. Vac. Sci. Technol. A* **1990**, *8*, 3449.
[42] P. De Wolf, R. Stephenson, T. Trenkler, T. Clarysse, T. Hantschel, W. Vandervorst, *J. Vac. Sci. Technol. B.* **2000**, *18*, 361.
[43] M. Hage-Ali, R. Stuck, A. N. Saxena, P. Siffert, *Appl. Phys.* **1979**, *19*, 25.

  